Gas-Phase Study of the Chemistry and Coordination of Lead(II) in the Presence of Oxygen-, Nitrogen-, Sulfur-, and Phosphorus-Donating Ligands

Ljiljana Puskar, Perdita E. Barran,[†] Bridgette J. Duncombe,[‡] Daniel Chapman, and Anthony J. Stace*[,‡]

Department of Chemistry, University of Sussex, Falmer, Brighton BN1 9QJ, United Kingdom

Received: June 1, 2004; In Final Form: October 20, 2004

Using a pickup technique in association with high-energy electron impact ionization, complexes have been formed in the gas phase between Pb^{2+} and a wide range of ligands. The coordinating atoms are oxygen, nitrogen, sulfur, and phosphorus, together with complexes consisting of benzene and argon in association with Pb^{2+}. Certain ligands are unable to stabilze the metal dication, the most obvious group being water and the lower alcohols, but CS_2 is also unable to form $[Pb(CS_2)_N]^{2+}$ complexes. Unlike many other metal dication complexes, those associated with lead appear to exhibit very little chemical reactivity following collisional activation. Such reactions are normally promoted via charge transfer and are initiated using the energy difference between $M^{2+} + e^- \rightarrow M^+$ and $L \rightarrow L^+ + e^-$, which is typically ∼5 eV. In the case of Pb^{2+}, this energy difference usually leads to the appearance of L^+ and the loss of a significant fraction of the remaining ligands as neutral species. In many instances, Pb^+ appears as a charge-transfer product. The only group of ligands to consistently exhibit chemical reactivity are those containing sulfur, where a typical product might be $PbS^+(L)_M$ or $PbSCH_3^+(L)_M$.

Introduction

The behavior of divalent lead, Pb(II), with respect to biological materials is well-documented.[1−4] The metal is known to cause rapid degradation of RNA, where a Pb(II)-induced catalytic reaction sequence leads to the cleavage of a sugar−phosphate link.[5] Similarly, Pb^{2+} has been shown to inhibit the action of Zn(II) metalloenzymes,[6,7] and the ion is also known to replace Ca^{2+} in bone tissue.[8] All these factors make it desirable to try and understand the chemistry of Pb^{2+} and to investigate how the binding sites on individual molecules might interact with the ion to give stable coordination units.

The coordination of Pb^{2+} is complicated by the presence of a $6s^2$ electron lone pair on the ion. Due to a relativistic contraction of the 6s orbital, these electrons are comparatively strongly bound to the nucleus,[9] which makes their displacement or participation in bonding energetically unfavorable. The net result is a lone pair that both is chemically inert and can have a stereochemical influence on the disposition of ligands.[4,10] Both holodirected (uniform) and hemidirected (nonuniform) complexes have been identified,[4,10] with the latter being associated with an identifiable void in the displacement of ligands surrounding Pb^{2+}.[11]

Presented here are the results of a study of the chemistry and coordination of Pb^{2+} in the gas phase. By studying a wide range of $[PbL_N]^{2+}$ complexes, it is possible to comment on the ability of L to stabilize the ion with respect to charge transfer. In addition, observations on variations in the size of stable complexes can reveal details of preferred coordination numbers. Through these experiments, it has been possible to explore a wide range of molecular environments in association with Pb^{2+}, and coordination has been examined in the presence of O-, S-, N-, and P-donor ligands. These experiments are part of a series that have been initiated through the successful development of a pickup technique for preparing multiply charged metal−ligand complexes in the gas phase.[12−16] Salpin and Tortajada have been successful in using electrospray to achieve similar objectives with Pb(II);[17,18] however, the pickup technique would appear to be the only method capable of preparing Pb(II)-based complexes where the metal cation is associated with a very wide range of ligands.

Experimental Section

The experimental setup has been described in detail elsewhere. Lead pellets (Sigma-Aldrich) in an effusive source (DCA Instruments) are held at between 900 and 950 °C, to yield $\sim 10^{-2}$ mbar of lead vapor. This region is crossed with a neutral beam of mixed ligand−argon clusters (L_NAr_M), which are formed by the adiabatic expansion of a vapor/argon mixture through a pulsed supersonic nozzle. The clusters pass through a 1 mm diameter skimmer into the path of the metal vapor, where the mixed solvent−argon clusters pick up lead atoms. These neutral clusters then enter the ion source of a high-resolution double-focusing mass spectrometer (VG ZAB-E), where they are ionized by electron impact at 100 eV. In combination with the thermal pickup process, ionization is thought to cause complete evaporation of the rare gas atoms from the clusters (no ions of the form $[Pb(L)_NAr_M]^{Z+}$ are detected). Previous experiments have indicated that the presence of rare gas atoms as an energy sink is essential to the pickup process.[19]

A shutter situated at the top of the oven enables an unambiguous assignment of signals due to metal-containing species, and values recorded for parent and fragment ion intensities represent differences between shutter open and closed signals; this step is necessary since ligand clusters dominate

[†] Present address: School of Chemistry, Joseph Black Building, West Mains Road, Edinburgh EH9 3JJ, U.K.

[‡] Present address: School of Chemistry, The University of Nottingham, University Park, Nottingham NG7 2RD, U.K.

10.1021/jp047637f CCC: $30.25 © 2005 American Chemical Society
Published on Web 12/10/2004

TABLE 1[a]

ligand	IE/eV	α/Å^3	μ/D	lead N_{min}	lead N_{max}	lead [Pb(ligand)$_N$]$^{2+}$
Oxygen-Containing						
water	12.61	1.45	1.85			no stable 2+ complexes (hydroxide only)
methanol	10.85	3.29	1.47			no stable 2+ complexes (alkoxide only)
ethanol	10.47	5.41	1.69			no stable 2+ complexes (alkoxide only)
1-propanol	10.22	6.74	1.58	3		NL and CTL (alkoxide formation)
1-butanol	9.99			3		NL and CTL (alkoxide formation)
acetone	9.70	6.39	2.7	2	4-6	NL and CTL
carbon dioxide	13.77	2.91	0	1	4-6	NL and CTL
furan	8.85			2	3-5	NL and CTL
1,2-dimethoxyethane	9.30			2	3	NL and reactions
Nitrogen-Containing						
ammonia	10.16	2.26	1.47			no stable 2+ complexes
acetonitrile	12.2	4.4	3.44	1	3	NL, CTL, and reactions
pyridine	9.26	9.5	2.2	1	3	NL, CTL, and limited reactivity
ethylenediamine	9.25		1.9	1	1	only forms [PbL]$^{2+}$
pyrrole	8.64	9.27	4.22	2	3	NL and CTL
Sulfur-Containing						
thiophene	8.86			2	2	NL, CTL, and reactions
dimethyl sulfide	8.69			3	3	NL, CTL, and reactions
ethylene sulfide	9.05			2	3	NL, CTL, and reactions
CS_2	10.08		0			no stable 2+ complexes
Phosphorus-Containing						
tert-butylphosphaalkyne ($Bu^tC{\equiv}P$)	9.61			3	5?	NL and CTL
Miscellaneous						
benzene	9.24	10.32	0	2	2	NL and CTL
argon	15.76	1.6	0	1	?	NL and CTL

[a] Key: IE, ionization energy; σ, polarizability; μ, dipole moment; NL, neutral ligand loss; CTL, charge transfer accompanied by the loss of charged and neutral ligands; N_{min}, the lowest value of N for which a stable [Pb(L)$_N$]$^{2+}$ complex was observed; N_{max}, the value for N at which the relative intensities of [Pb(L)$_N$]$^{2+}$ complexes reached a maximum.

the total ion signal. Information on fragmentation was obtained by studying both the unimolecular and collision-induced dissociation (CID) of size-selected complexes. For the smaller [Pb(L)$_N$]$^{2+}$ ions, collision-induced fragmentation pathways are dominated by charge-transfer processes, and for the purposes of promoting the latter, the background pressure in a cell situated next to the single focusing slit in the second field free region of the mass spectrometer is increased to approximately 10^{-6} mbar. Reaction products are identified by systematically scanning the voltage of the electrostatic analyzer,[20] a procedure that results in a mass-analyzed ion kinetic energy (MIKE) spectrum.

Results and Discussion

The coordination chemistry of Pb(II) has been discussed at length in a recent paper by Shimoni-Livny et al. and in a review by Claudio et al. In particular, these papers highlight the distinction between holo- and hemidirected complexes in terms of differences in coordination number. As might be expected, the stereochemical influence of the 6s^2 lone pair results in hemidirected complexes having, on average, lower coordination numbers than the holodirected complexes. Table 1 presents a summary of the ligands studied (successes and failures) together with details of those physical properties (dipole moment and polarizability) of the ligands that may be relevant to any discussion on the stability of a particular [PbL$_N$]$^{2+}$ complex. The term "ligand" is used in a very loose sense because some of the complexes that have been prepared, for example, those with a rare gas, such as [PbAr$_N$]$^{2+}$, can only exist under the collision-free conditions present in our experiment. However, it is interesting to note that transition metal ion−rare gas complexes of the type seen in previous experiments[21] have been prepared in the condensed phase.[22] The discussion that follows highlights details from a selection of the complexes studied.

For certain ligands, it is possible to make comparisons with results obtained for other metal dications.[13,14,16,23−28] In many instances, the collisional activation of a complex promotes charge transfer, and this step is often accompanied by chemical reactivity of the ligand, which gains energy from the difference in ionization energies (see Table 1). If this energy difference were the only factor, then the results from Mg^{2+} (second IE = 15.03 eV),[14,26,28] Mn^{2+} (second IE = 15.64 eV),[24,26,28,29] and Zn^{2+} (second IE = 17.96 eV)[26,30] might be expect to be very similar to those reported here for Pb^{2+}, where the second IE is 15.03 eV. However, as will be seen, Pb^{2+} promotes very little fragmentation in many of the ligands studied.

Oxygen-Based Ligands. As noted in an earlier paper,[31] there is a series of related molecules for which Pb(II) complexes are unstable with respect to charge transfer. These molecules are water, methanol, and ethanol, and the only stable ions observed are the hydrolysis or alkolysis products, i.e., $Pb^+OH(H_2O)_N$ or $Pb^+OR(ROH)_N$. Only when R = $CH_3CH_2CH_2$ does the corresponding doubly charged complex become stable and appears in a mass spectrum.[31] The Pb(II) cation is considerably more acidic than its charge/size ratio would suggest, and this anomalous pK_a is only matched once the basicity of the alcohol increases to that of propanol. Details of the fragmentation patterns of [Pb(ROH)$_N$]$^{2+}$ clusters are not presented here but can be found in ref 31. A recent paper by Cox and Stace addresses the acidity of Pb^{2+} from a theoretical viewpoint[32] and concludes that high acidity is promoted when proton transfer occurs early on along the reaction coordinate where the energy barrier is at its lowest. In a very recent paper,[33] Bohme and co-workers have succeeded in preparing the doubly charged monohydrate, [Pb·H_2O]$^{2+}$, via an exchange reaction, which resulted in trapping the species in a metastable state below the charge-transfer barrier. It remains to be seen if this technique

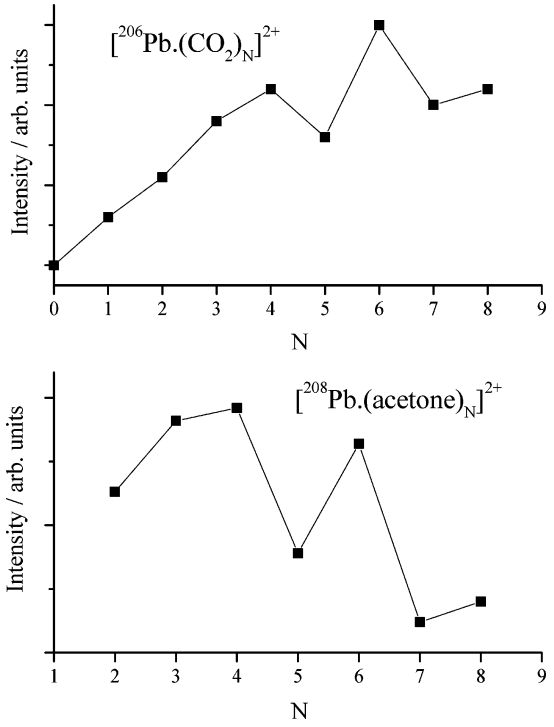

Figure 1. Parent ion intensity distributions for $[^{208}Pb(CO_2)_N]^{2+}$ and $[^{208}Pb(acetone)_N]^{2+}$ complexes. Profiles with very similar shapes have been recorded for isotopes of lead other than those shown.

can yield ions containing more than one water molecule. Calculations presented earlier[32] would suggest that the charge-transfer barriers for these ions are comparatively low.

Figure 1 shows relative intensity data recorded for two systems, $[^{208}Pb(CO_2)_N]^{2+}$ and $[^{208}Pb(\{CH_3\}_2CO)_N]^{2+}$, plotted as a function of *N*. In each case the results for just one isotope of lead (^{208}Pb) are shown; however, data recorded for other isotopes follow very similar trends. In all of the examples given below, reproducibility is gauged primarily through the use of repeat measurements on the lead isotopes ^{206}Pb, ^{207}Pb, and ^{208}Pb, but, in most instances, only one set of data is plotted. The profiles of the intensity distributions recorded for $[^{208}Pb(CO_2)_N]^{2+}$ and $[^{208}Pb(\{CH_3\}_2CO)_N]^{2+}$ as a function of *N* are remarkably similar to the composite diagram presented by Shimoni-Livny et al.[10] for Pb(II) coordination in the condensed phase (Chart 1 of ref 10). The latter is derived from data available on the Cambridge Structural Database[34] and shows the most frequent coordination numbers to be 4 and 6, with a distinct absence of five-coordinate structures. The chart given by Shimoni-Livny et al. is also a composite of both hemi- and holodirected structures. A detailed discussion of how CO_2 molecules might bond to Pb^{2+} is given below, where these results are compared with those recorded using CS_2 as a ligand.

The nature of the experiment discussed here is such that complexes containing any number of ligands (1−50) can be prepared and sometimes observed.[35] However, there are quite often distinct trends in behavior that give rise to particularly intense ion−ligand combinations, which might otherwise be labeled as "magic numbers". There are arguments for and against the correlation of magic numbers with stable structures—the supporting *rationale* being that the conditions leading to the formation of ions (of any composition) are sufficiently violent as to leave the $[Pb(L)_N]^{2+}$ species with large amounts of internal energy. During the course of their passage through the apparatus ($\sim 10^{-4}$ s), comparatively unstable ions fragment, while ions that encounter a high reaction barrier (dissociation energy) do not. Since these are nonequilibrium experiments, reactivity proceeds in one direction only, which is fragmentation downward from large-sized complexes. The net result is a "distillation" of sizes, where stable complexes gain in intensity at the expense of those that are less stable.

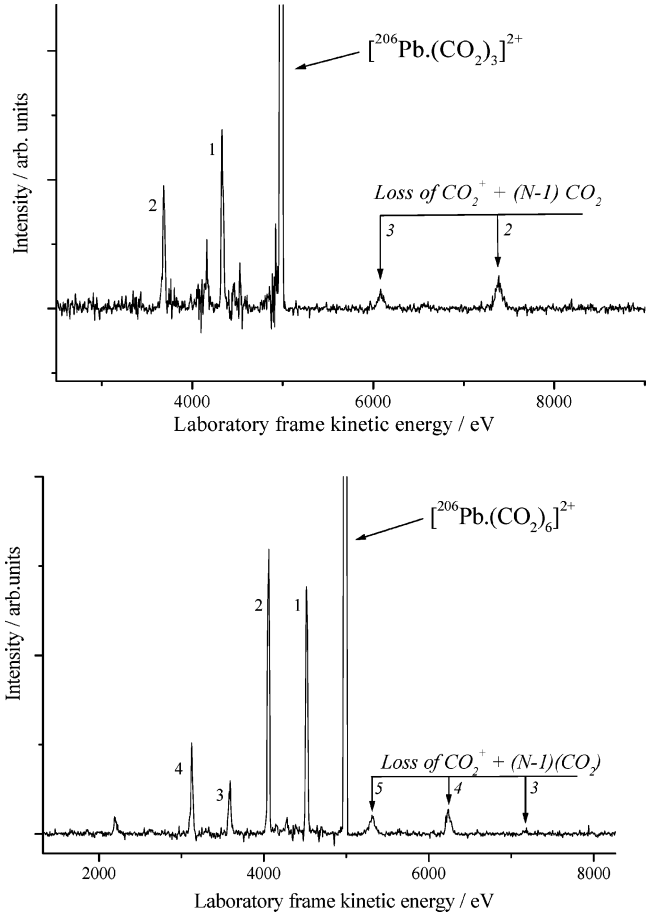

Figure 2. Fragmentation patterns of $[^{206}Pb(CO_2)_N]^{2+}$ complexes for $N = 3$ and 6 following collisional activation. The values shown correspond to the numbers of neutral ligands lost as a consequence of collisional activation, with features associated with charge-transfer processes being shown in italics. For certain values of *N* there is a mass coincidence with an underlying singly charged ion, which, in the case of $N = 6$, is responsible for the unexpected alternation in neutral ligand loss from the doubly charged ion.

A quantitative example of how this process works is to be found in recent experiments and calculations on $[Cu(pyridine)_N]^{2+}$ and $[Ag(pyridine)_N]^{2+}$ complexes.[36,37] The UV photoexcitation ($h\nu = 4.6$ eV) of either complex for *N* in the range of 5−8 always gives >90% $N = 4$ as the product ion.[36] Complementary calculations on both complexes show the incremental binding energy at $N = 4$ to be $\sim$100 kJ mol^{-1} greater than either $N = 3$ or $N = 5$.[37] Thus, we would conclude that, in our type of experiment, high-energy ions preferentially fragment to stable (magic number) structures.

Figure 2 shows two examples of CID fragmentation patterns recorded for $[^{208}Pb(CO_2)_N]^{2+}$ complexes, where $N = 3$ and 6, and Figure 3 shows the corresponding results obtained for $[^{208}Pb(\{CH_3\}_2CO)_{3,6}]^{2+}$ complexes. In each of the MIKE scans there are two sets of prominent features: narrow peaks arising from the loss of neutral ligand molecules from each of the ions and broader peaks, which denote that a release of kinetic energy accompanies these particular fragmentation processes. These latter peaks arise from charge transfer, and the kinetic energy release is due to Coulomb repulsion between the separating

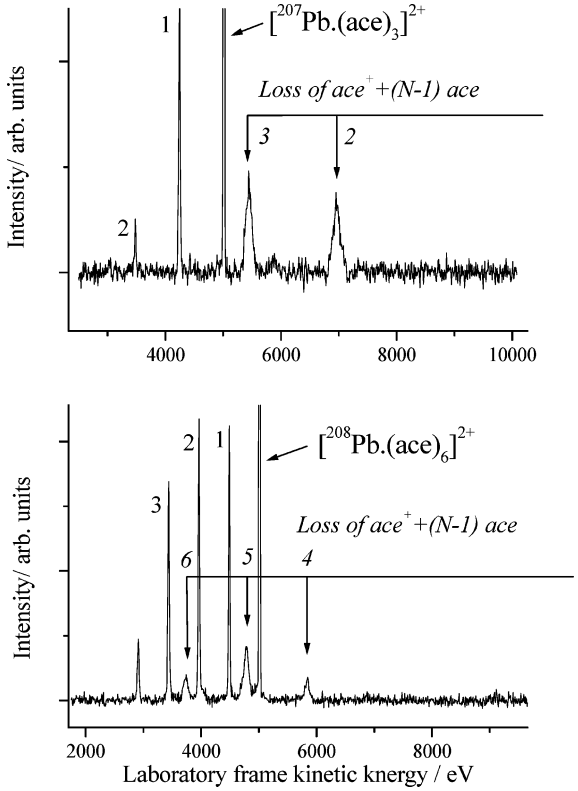

Figure 3. Fragmentation patterns of $[Pb(acetone)_N]^{2+}$ complexes for $N = 3$ and 6 following collisional activation. Charge-transfer processes are shown in italics.

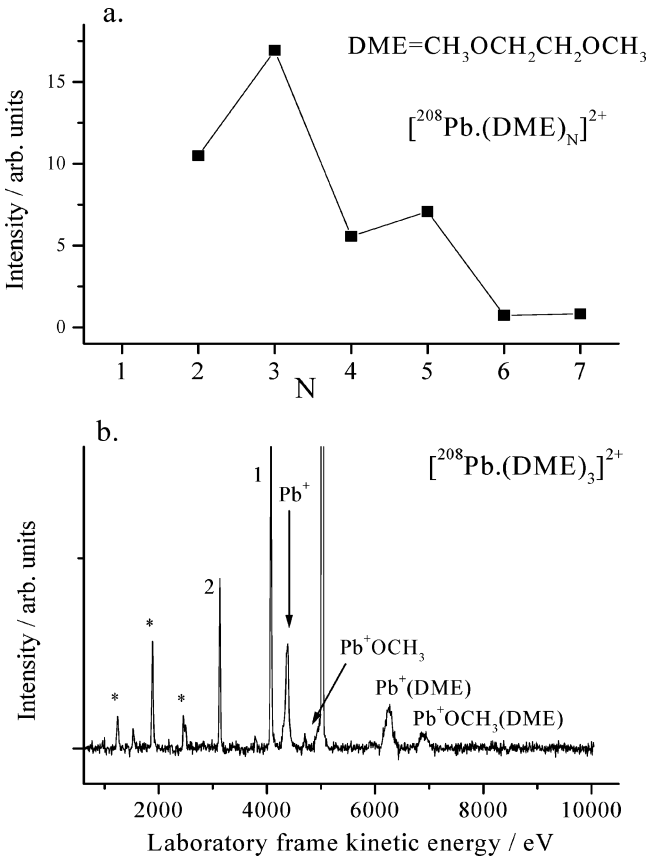

Figure 4. (a) Parent ion intensity distribution for $[^{208}Pb(DME)_N]^{2+}$ complexes and (b) fragmentation pattern recorded for $[^{208}Pb(DME)_3]^{2+}$ following collisional activation. The peaks denoted by asterisks (∗) are fragments from an underlying ion with the same nominal mass as $[^{208}Pb(DME)_3]^{2+}$.

charges. Two features to these data are worthy of note. First, the charge-transfer peaks involving CO_2 are narrower than those associated with acetone complexes. This difference is primarily due to the much higher ionization energy of CO_2 compared with acetone (see Table 1), and therefore the energy difference between each ligand and the second ionization energy of lead is much smaller for CO_2 than for acetone. A second feature of the results (and this statement applies to many of the ligands discussed below) is the almost total absence of any evidence of molecular fragmentation as a result of charge transfer. In addition to promoting a release of kinetic energy, Coulomb repulsion can also lead to internal excitation in molecular ions that, in some instances, results in fragmentation. In the case of CO_2, charge transfer in $[Cu\ (CO_2)_N]^{2+}$ complexes leads to the appearance of products containing CuO^+, and for acetone the charge-transfer product $CH_3COCH_3^+$ can form $CH_3CO^+ + CH_3$ with the latter neutral fragment remaining attached to the reduced metal cation.[16,29,30]

Experiments involving Pb^{2+} in association with furan resulted in the formation of stable complexes, which exhibited both neutral and charge-transfer loss of molecules following collisional excitation. The final oxygen-based ligand to be studied was 1,2-dimethoxyethane (DME = $CH_3OCH_2CH_2OCH_3$) with which it was hoped Pb^{2+} might form a bidentate complex. Figure 4a shows the distribution of relative intensities for $[^{208}Pb(DME)_N]^{2+}$ complexes as a function of N, and Figure 4b shows the result of a CID experiment on $[^{208}Pb(DME)_3]^{2+}$. For bidentate behavior the intensity distribution might have been expected to peak at either $N = 2$, 3, or 4. However, distributions similar to that shown in Figure 4a have also been recorded for other large ligands, where there is only one obvious site for coordination, e.g., pyridine. In contrast to the behavior shown in Figure 4a, the intensity distribution recorded for singly charged complexes, $[^{208}Pb(DME)_N]^+$, peaks at $N = 1$; however, this pattern is also similar to that displayed by most singly charged complexes. Interestingly, DME is one of the few oxygen-containing ligands to exhibit significant fragmentation in association with Pb^{2+}; indeed, charge transfer promotes total reactivity, with no evidence of the formation of the singly charged ligand, DME^+, in any of the MIKE spectra. Figure 4b shows fragments corresponding to the formation of Pb^+OCH_3, but bidentate behavior might also have been expected to lead to the observation of $Pb^+(OCH_3)_2$ as a charge-transfer product; however, there is no evidence of such a fragment in any of the CID scans.

Nitrogen-Based Ligands. No stable complexes could be found between Pb^{2+} and ammonia. Given the ease with which oxygen-based hydrogen-bonded solvents underwent hydrolysis, it is not too surprising that ammonia was observed to be similarly unstable with respect to clustering with Pb^{2+}. However, ammonia is a much stronger base than any of the alcohols studied, and, therefore, taking into consideration earlier conclusions regarding the Lewis acid character of Pb^{2+}, stable $[Pb(NH_3)_N]^{2+}$ complexes might have been anticipated. In contrast, most aprotic nitrogen-based solvents readily formed stable complexes with the lead dication. A distribution of the relative intensities of $[Pb(CH_3CN)_N]^{2+}$ complexes as a function of size is shown in Figure 5, and Figure 6 shows the results from two MIKE scans following the collisional activation of $[Pb(CH_3CN)_4]^{2+}$ and $[Pb(CH_3CN)_6]^{2+}$. Both sets of results show evidence of quite extensive charge transfer, frequently accompanied by fragmentation, which, as stated earlier, appears to be unusual for Pb(II) complexes. The dominant decay pathways are as follows:

$$[Pb(CH_3CN)_N]^{2+} \rightarrow [Pb(CH_3CN)_{N-K}]^{2+} + K(CH_3CN) \quad (1)$$

$$[Pb(CH_3CN)_N]^{2+} \rightarrow Pb[(CH_3CN)^+]_{N-K} + CH_3CN^+ + (K-1)CH_3CN \quad (2)$$

$$[Pb(CH_3CN)_N]^{2+} \rightarrow PbCN^+(CH_3CN)_{N-K} + [CH_3 + (K-1)CH_3CN]^+ \quad (3)$$

For reaction 3 the nonmetallic products are bracketed together since, in the absence of observing the counterion, it is uncertain as to where the charge resides. This same notation is used in all subsequent figures to denote processes where charge transfer is accompanied by chemical reactivity, but where the location of the charge on the nonmetal component has yet to be established. There is insufficient resolution to tell if the product acetonitrile ion from charge transfer takes the form of either CH_3CN^+ or H^+CH_3CN. However, on the basis of the results from experiments by other groups who have examined complexes involving CH_3CN associated with alkaline earth and transition metals,[23−26] both products might be expected. The decay patterns also show extensive loss of neutral acetonitrile (reaction 1) down to the minimum observed size, which in this case is $[Pb(CH_3CN)]^{2+}$. From a purely electrostatic viewpoint,[14,15] the high ionization energy of the ligand, combined with a large dipole moment, would appear to minimize the probability of charge transfer and facilitate the ability of the metal dication to form a stable complex with just a single ligand. One feature that is common to many of the fragmentation patterns is that the charge-transfer process frequently removes all the ligands from the metal ion to yield a prominent peak corresponding to Pb^+.

In contrast to the modest degree of fragmentation seen for $[Pb(CH_3CN)_N]^{2+}$ complexes, the collisional activation of $[Pb(pyridine)_N]^{2+}$ shows pyridine$^+$ to be the only charge-transfer product. In particular, there is no evidence of ions of the form $MCN^+(pyridine)_K$ as seen by Shvartsburg[28] when fragmentation of the ring is induced by charge transfer. Both Mg^{2+} and Mn^{2+} in association with pyridine show evidence of extensive ring destruction leading to the appearance of, for example,[28,29,38] $MnCN^+(pyridine)_K$ ions; in contrast, such behavior could not be detected in $[Pb(pyridine)_N]^{2+}$ complexes.

Attempts to coordinate Pb^{2+} with bidentate nitrogen-based ligands met with mixed success. Although comparatively intense ion signals could be detected for singly charged Pb^+ in association with both ethylenediamine (EN) and *N*,*N*,*N*′,*N*′-tetramethylethylenediamine (TMED), the only doubly charged complex that could be observed was $[Pb(EN)]^{2+}$. Collisional activation of this ion resulted in the charge-transfer products Pb^+ and EN^+.

Sulfur-Based Ligands. The rationale behind many of the recent condensed-phase experiments on the chemistry of lead−sulfur compounds has been the possibility of developing a lead-selective sequestering agent as a means of controlling the toxicity of the metal.[39,40] Such experiments have demonstrated the importance of understanding the coordination of Pb^{2+} to sulfur-based ligands,[41] which are considered to be "softer" than those containing either oxygen or nitrogen. Lead-specific sequestering compounds should be capable of matching the Lewis acidity of the metal, which, as we have already demonstrated, can result in charge transfer when the circumstances are not favorable. Given the variation in "hardness" between oxygen- and sulfur-containing ligands, a good example of how this difference might influence events should come from

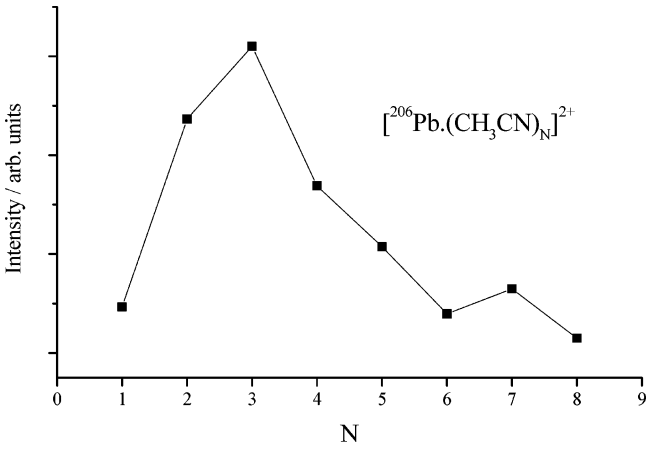

Figure 5. Distribution of relative intensities for $[^{206}Pb(CH_3CN)_N]^{2+}$ complexes plotted as a function of *N*.

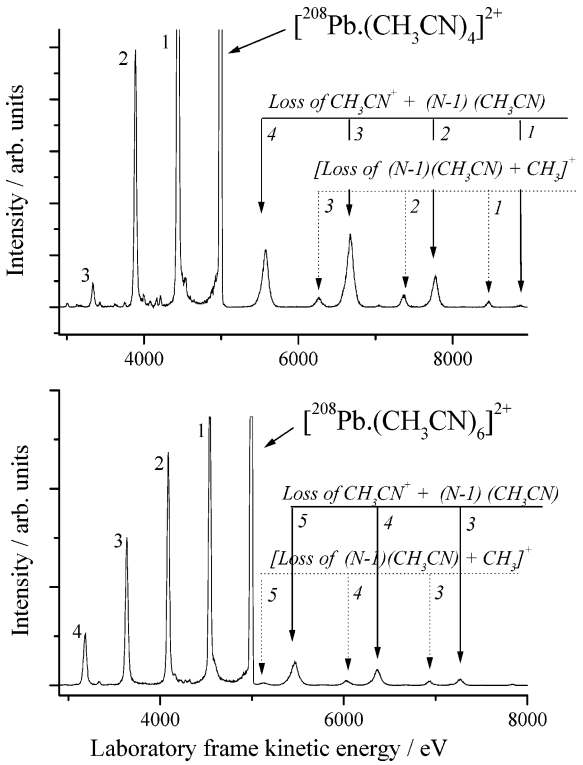

Figure 6. Fragmentation patterns recorded for $[^{208}Pb(CH_3CN)_N]^{2+}$ complexes for $N = 4$ and 6 following collisional activation. Charge-transfer processes are shown in italics.

a comparison of CO_2 with CS_2. As already demonstrated, the former readily stabilizes Pb^{2+} to give a series of ions of the form $[Pb(CO_2)_N]^{2+}$ for *N* in the range of 1−9. In contrast, no analogous $[Pb(CS_2)_N]^{2+}$ ions are observed for any value of *N*. This is not a failure of the pickup process because there is an abundance of singly charged ions of the form $Pb^+(CS_2)_N$, which is confirmed in Figure 7, where a MIKE scan recorded following the collisional activation of $Pb^+(CS_2)_3$ is shown. These data also serve to illustrate the type of fragmentation pattern we might expect to see when a sulfur-containing ligand is coordinated to a cation. Of particular interest are the appearance of Pb^+S and $Pb^+(CS)$, which are both consistent with the products observed from previous studies of ion−molecule reactions between singly charged metal ions and individual CS_2 molecules.[42,43]

Both experiment and theory suggest a number of ways in which CS_2 and CO_2 could coordinate to a metal.[42−45] For a single molecule, the options are as follows: η^1, end-on

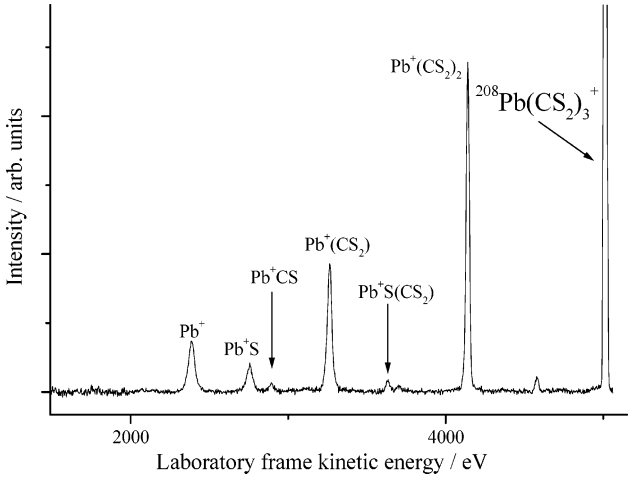

Figure 7. Fragmentation pattern recorded for the singly charged ion, $[^{208}Pb(CS_2)_3]^+$, following collisional activation. This observation was made in order to confirm that the absence of $[Pb(CS_2)_N]^{2+}$ complexes was not due to a failure of the pickup process.

coordination; η^1, C coordination; and η^2, side-on coordination. There also exists the possibility that molecules may form bridged structures, but these normally require the participation of additional atoms, which serve to stabilize the exposed carbon and/or sulfur atoms. Calculations by Jeung[46] suggest a further geometric option, η^3_{SCS}, where all three atoms are wrapped around a metal atom. For several neutral metal atoms, this geometry is calculated to be more stable than either η^1 or η^2 coordination. In contrast, calculations by Sakaki et al.[47] show that for Cu(I) with CO_2, the end-on η^1 configuration is favored because of electrostatic interactions. With Pb(II) being doubly charged and a negative charge on each of the terminal O atoms, electrostatic interactions should favor the η^1 end-on coordination for CO_2. The other modes of coordination appear to require metal-to-ligand electron transfer, which in our case would be unlikely because Pb(II) has a $5d^{10}6s^2$ closed-shell configuration. The failure to observe $[Pb(CS_2)_N]^{2+}$ complexes would suggest that, for CS_2, electrostatic interactions alone are not sufficient to bind the ligand to the metal dication. In addition, electron transfer between the sulfur atom on CS_2 and Pb(II) to form the type of covalent interactions that is considered characteristic of a "soft metal−soft ligand" system[48] may not be sufficient because of additional electronegativity of sp^2 sulfur atoms (as opposed to the sp^3 character of the successful S-containing ligands discussed below). Finally, the enhanced reactivity of CS_2 compared with CO_2 could also be a contributing factor in the instability of a complex. Calculations show that Fe^+ reacts with CS_2 by an insertion reaction to give FeS^+ and $FeCS^+$ as products and that an intermediate configuration on the reaction pathway adopts η^2 side-on coordination. Attempts to form such a geometry with Pb(II) would probably fail because of insufficient electron transfer; however, a similar coordination geometry could account for the appearance of PbS^+ and $PbCS^+$ from the Pb(I) complexes. Experiments comparing Zn(I) and Zn(II) in the presence of CO_2 and CS_2 show that, in terms of forming stable complexes, the $3d^{10}$ closed-shell Zn^{2+} cation behaves in a manner similar to Pb^{2+}. However, Zn^{2+} is far more reactive than Pb^{2+}.

As with the CO_2 and CS_2, thiophene (C_4H_4S) has the potential to attach to a metal in a variety of possible orientations.[49,50] The two most obvious are where the ligand adopts either η^1 geometry through a preference for σ bonding between a metal and an unbound electron pair on the heteroatom or a metal atom can participate in π bonding with the ring electrons and the

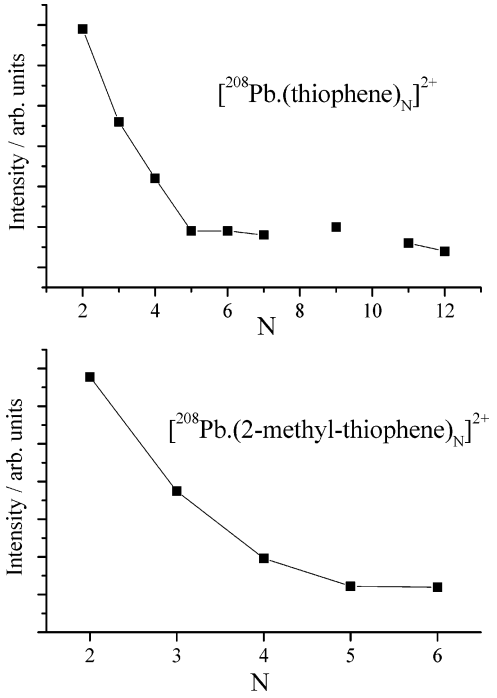

Figure 8. Distribution of relative intensities for $[^{208}Pb(thiophene)_N]^{2+}$ and $[^{208}Pb(2\text{-methylthiophene})_N]^{2+}$ complexes plotted as a function of N.

resultant complex adopts η^5 geometry. Figure 8 shows a plot of the relative intensities of $[Pb(C_4H_4S)_N]^{2+}$ complexes, where it can be seen that the most intense ions correspond to $N = 2$. To confirm this pattern of behavior, the experiments were repeated with 2-methylthiophene, and these results are also shown in Figure 8. Both profiles are very similar to those seen previously for complexes involving benzene (see also below), where two molecules in association with a metal cation form a stable sandwich structure.[13,16] Supporting this conclusion are the results of MIKE spectra recorded following the collisional activation of the thiophene complexes. The loss of neutral molecules from $[Pb(C_4H_4S)_N]^{2+}$ and the corresponding 2-methylthiophene complexes stops abruptly once $N = 2$. Further fragmentation does occur, but via charge-transfer processes involving $C_4H_4S^+$; some of the MIKE spectra consistently show the presence of very weak features corresponding to the formation of PbS^+ and $PbS^+(C_4H_4S)$.

Previous observations by a number of groups on the association of benzene with M^+ cations have shown the complexes to have a strong propensity to adopt sandwich structures.[51−53] Indeed, for a number metal dications, the $[M(C_6H_6)_2]^{2+}$ ion is the only stable species observed,[13,16] with the sandwich structure deriving stability from a strong electrostatic interaction between the doubly charged cation and the π electron system of the benzene molecule. The observation of a comparatively intense signal for $[Pb(C_4H_4S)_2]^{2+}$ could be interpreted as being due to a similar $M^{2+}-\pi$ interaction, resulting in the formation of a stable sandwich structure. This behavior can be compared with that of furan, where from Table 1 it can be seen that $[Pb(C_4H_4O)_N]^{2+}$ complexes have intensity maxima at $N = 3$ and 5, i.e., a pattern of behavior similar to that seen for other σ bonding complexes.

Differences in bonding preference between thiophene and furan are going to be influenced by the electronegativity of the heteroatom and/or the degree of lone pair delocalization through adjacent π bonds. The removal of electron density away from a heteroatom being responsible for enhanced π bonding at the

expense of the ligand being able to form σ bonds. Thiophene is generally considered to be a poor σ bonding ligand;[49,50] however, η^1 complexes are known and derive their stability from a bent configuration that enhances π bonding between the ring and vacant orbitals on the metal atom.[49,50] When thiophene acts as a η^5 ligand, it does so most efficiently with 4d and 5d metals. In contrast, furan is generally considered to favor σ bonding, although examples of η^5 complexes are known. At a qualitative level, the differences in behavior between furan and thiophene can be attributed to the difference in electronegativity between O and S, and, generally, metal-containing complexes associated with furan have η^1 geometries because of the high electronegativity of the O atom. The lead dication is an ideal candidate for this type of comparison because it is a closed-shell $6s^2$ ion, which means that all interactions are going to be predominantly electrostatic. Some Pauli repulsion is expected between the s^2 electrons and the ligands, but this should be approximately equivalent for each of the two heterocycles.

Figure 8 shows the relative intensities of two further sulfur-containing complexes plotted as a function of size, namely, $[Pb(DMS)_N]^{2+}$ and $[Pb(ES)_N]^{2+}$ (DMS = dimethyl sulfide, EN = ethylene sulfide). In both cases, the profiles follow a pattern observed previously, where there is a maximum at $N = 3-4$, followed by a trough at $N \approx 5$, which is then followed by a further, smaller maximum at $N = 6-7$. These results would suggest that, in both cases, the sulfur atom is acting as the coordination site. As shown in Figure 9, the collisional activation of small $[Pb(DMS)_N]^{2+}$ complexes provides evidence of fragmentation in the form of the charge-transfer reaction:

$$[Pb(DMS)_N]^{2+} \rightarrow PbSCH_3^+(DMS)_{N-K-1} + [CH_3 + K(DMS)]^+ \quad (4)$$

Similarly, the collisional activation of $[Pb(ES)_N]^{2+}$ (shown in Figure 9) also promotes reactivity with the observation of the charge-transfer step:

$$[Pb(ES)_N]^{2+} \rightarrow PbS^+(ES)_{N-K-1} + [C_2H_4 + K(ES)]^+ \quad (5)$$

Overall, these results show that Pb(II) will readily coordinate with small sulfur-containing molecules. In the case of thiophene and related ligands, the results would suggest that the metal ion forms a η^5 complex with the ring π system. For dimethyl sulfide and ethylene sulfide it is more probable that the sulfur atom acts as the coordination site and that, as a consequence, these structures exhibit a high degree of chemical reactivity as a result of charge transfer. The success of dimethyl sulfide and ethylene sulfide, when compared with CS_2, probably derives from the fact the sulfur atoms have sp^3 hybridization, which makes them less electronegative and therefore capable of forming an interaction with the cation that has a higher degree of covalency (Figure 10).

Phosphorus-Based Ligand. Figure 11 shows an example of where an attempt has been made to generate a Pb^{2+} complex with a volatile phosphorus-containing compound (*tert*-butyl-phosphaalkyne (tcp), $\{CH_3\}_3C{\equiv}P$). The MIKE scan shows clear evidence of the loss of neutral tcp and of charge-transfer steps leading to the loss of tcp^+. What is not obvious from any of the recorded data is how the ligand is coordinated to the metal ion. Unlike acetonitrile (CH_3CN), the phosphorus atom in tcp is less electronegative than nitrogen and does not, therefore, carry a large negative charge.[54] Thus, there may be competition between carbon and phosphorus as to which atom binds to the cation; however, the fact that it appears possible to attach at least five molecules of tcp to Pb^{2+} would suggest that it is the less sterically hindered P atom that coordinates to the metal. As with many of the previous examples, this ligand also exhibits charge transfer accompanied by the complete loss of all the remaining neutral ligands to give Pb(I).

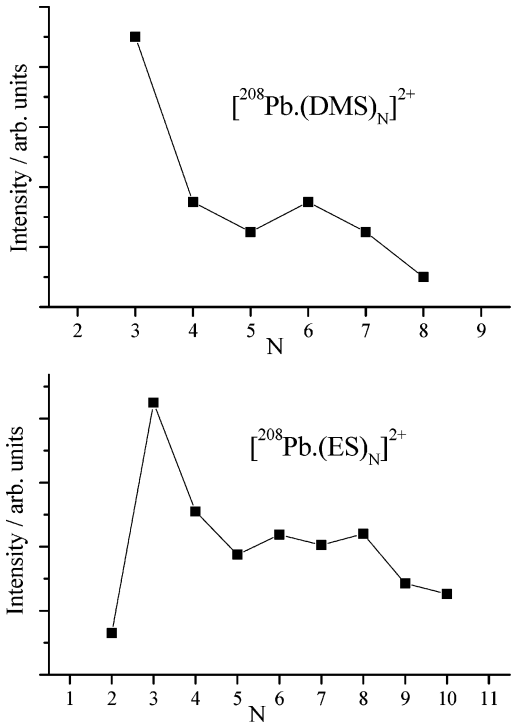

Figure 9. Distribution of relative intensities for [^{208}Pb(dimethyl sulfide)$_N$]$^{2+}$ and [^{208}Pb(ethylene sulfide)$_N$]$^{2+}$ complexes plotted as a function of *N*.

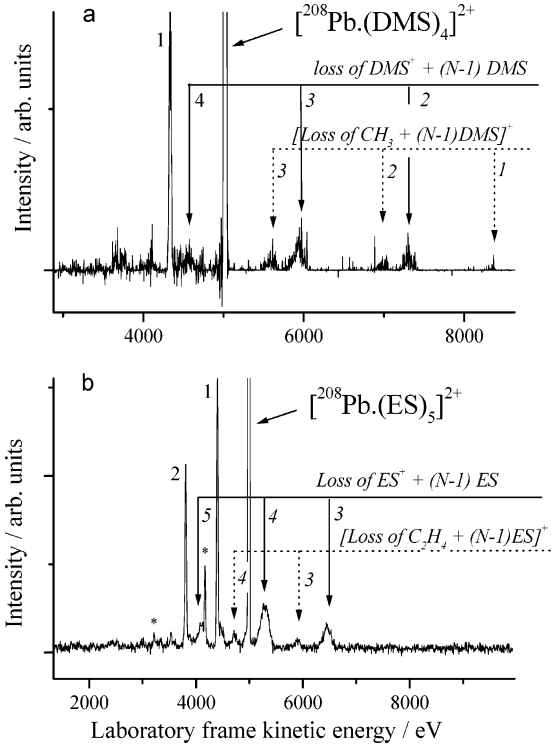

Figure 10. Fragmentation patterns recorded for (a) [^{208}Pb(dimethyl sulfide)$_4$]$^{2+}$ and (b) [^{208}Pb(ethylene sulfide)$_5$]$^{2+}$ following collisional activation.

Miscellaneous Ligands. Two other species that do not fall within the above categories have also been observed to bind

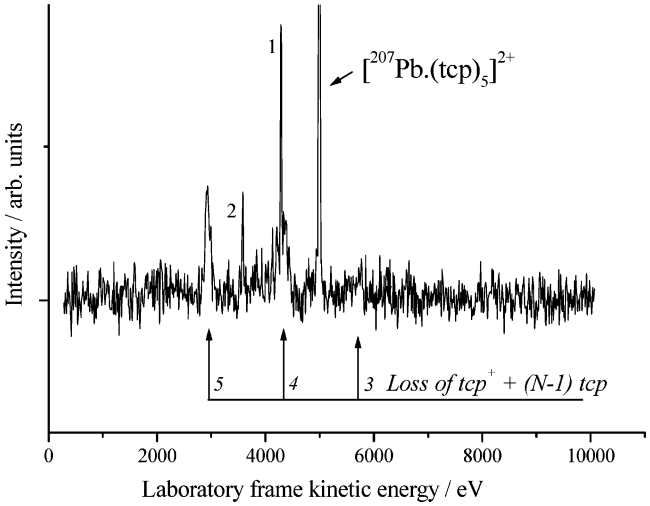

Figure 11. Fragmentation pattern recorded for $[^{207}Pb(\textit{tert}\text{-butylphosphaalkyne})_5]^{2+}$ following collisional activation.

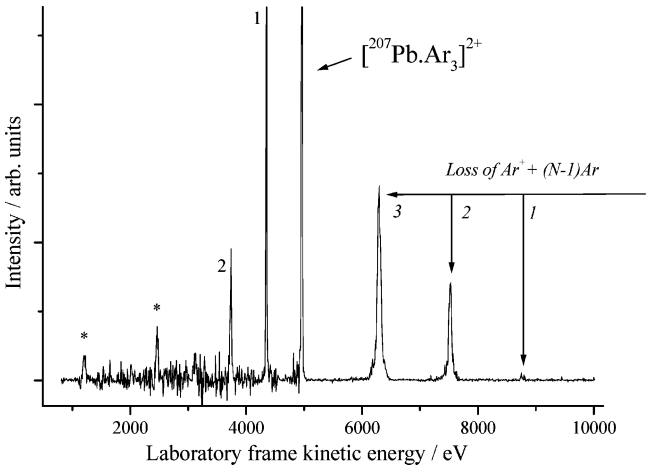

Figure 12. Fragmentation pattern recorded for $[^{207}PbAr_3]^{2+}$ following collisional activation.

with Pb^{2+} to form stable complexes, and these are argon and benzene. The $[Pb(Ar)_N]^{2+}$ system is slightly different from the other complexes considered above, in that the ionization energy of the ligand (Ar), at 15.76 eV, is higher that the second IE of lead. Therefore, it is highly likely in these complexes that a significant fraction of the 2+ charge remains on the metal cation. Evidence to this effect can be seen from the fact that the ion $[PbAr]^{2+}$ is stable, which would not normally be the case for a poor electron donor, such as argon. Figure 12 shows the result of a MIKE scan following the collisional activation of $[PbAr_3]^{2+}$. The most interesting features are the very narrow charge-transfer peaks, which confirm the very small difference in ionization energy between Pb^+ and argon.

The final complexes to be studied were those formed between Pb^{2+} and benzene. Figure 13a shows the first intensity profile recorded for $[Pb\ (Bz)_N]^{2+}$ complexes as a function of *N*. As can be seen, it is possible to form large solvation units, but for both isotopes of lead an interesting alternation in intensity occurs after $N = 7$. The reason for this behavior is a mass coincidence between, for example, $[^{208}Pb(Bz)_8]^{2+}$ (*m*/*z* 416) and $^{208}Pb_2^+$ (*m*/*z* 416). Under the conditions at which the oven is operated, the metal vapor contains a significant fraction of the lead dimer, Pb_2, which also displays a strong affinity for benzene clusters. It is also quite possible that sequential pickup is responsible for a significant fraction of the lead dimer signal. Although attempts were made to reduce the vapor pressure of gaseous

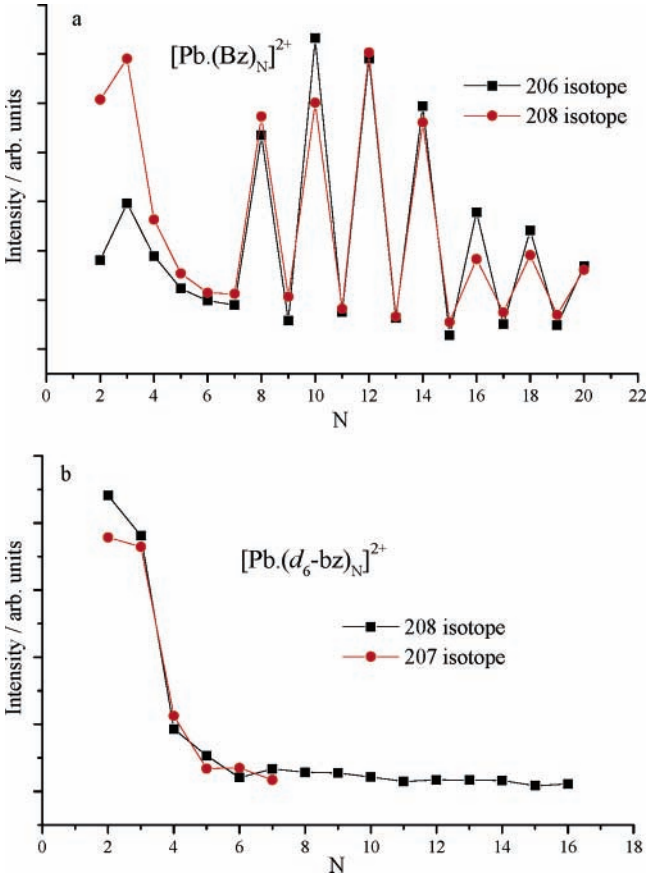

Figure 13. Intensity distributions recorded for (a) $[Pb(benzene)_N]^{2+}$ and (b) $[Pb(benzene\text{-}d_6)_N]^{2+}$ complexes, plotted as a function of *N*.

lead in the pickup region, it proved impossible to eliminate the presence of the dimer ion altogether. However, the coincidence problem is easily rectified using benzene-d_6, and Figure 13b shows the corresponding plot for Pb^{2+}/benzene complexes in the form of $[Pb(Bz\text{-}d_6)_N]^{2+}$. As might be expected, the distribution of ion intensities is dominated by the ion containing two benzene rings, which we take to be indicative of some form of sandwich structure.[51−53] Similar behavior has been observed on the part of other $[M(Bz)_N]^{2+}$ systems, and, in some instances, the $[M(Bz)_2]^{2+}$ ion is the only species observed.[13,16] However, that is not the case here; ions are observed out to $[Pb(Bz)_{20}]^{2+}$, and the comparatively high intensity of $[Pb(Bz)_3]^{2+}$ would suggest the presence of alternative structures to the traditional parallel sandwich. It is possible that the steric influence of the $6s^2$ lone pair has some effect on the structures of the smaller complexes.

Figure 14 shows two examples of MIKE spectra recorded following the collisional activation of $[Pb(Bz)_5]^{2+}$ and $[Pb(Bz\text{-}d_6)_9]^{2+}$. As seen in previous examples involving Pb^{2+}, there is evidence that, for the smaller ions, fragmentation is dominated by a very intense charge-transfer process, leading to a complete loss of ligands and the appearance of Pb^+. For $[Pb(Bz)_5]^{2+}$ the MIKE scan is dominated by the broad feature resulting from total fragmentation. From the corresponding experiment on $[Pb(Bz\text{-}d_6)_9]^{2+}$ complexes it can be seen that this process begins to tail off at $N = 8$. Overall, these observations would suggest that the high exothermicity of the charge-transfer process ($IE(C_6H_6) = 9.2$ eV) promotes the evaporation of neutral molecules from $Pb^+(C_6H_6)_K$ product ions and that benzene is not bound particularly strongly to the singly charged lead cation. A similar conclusion regarding coulomb-induced evaporation was reached following the collisional activation of doubly and

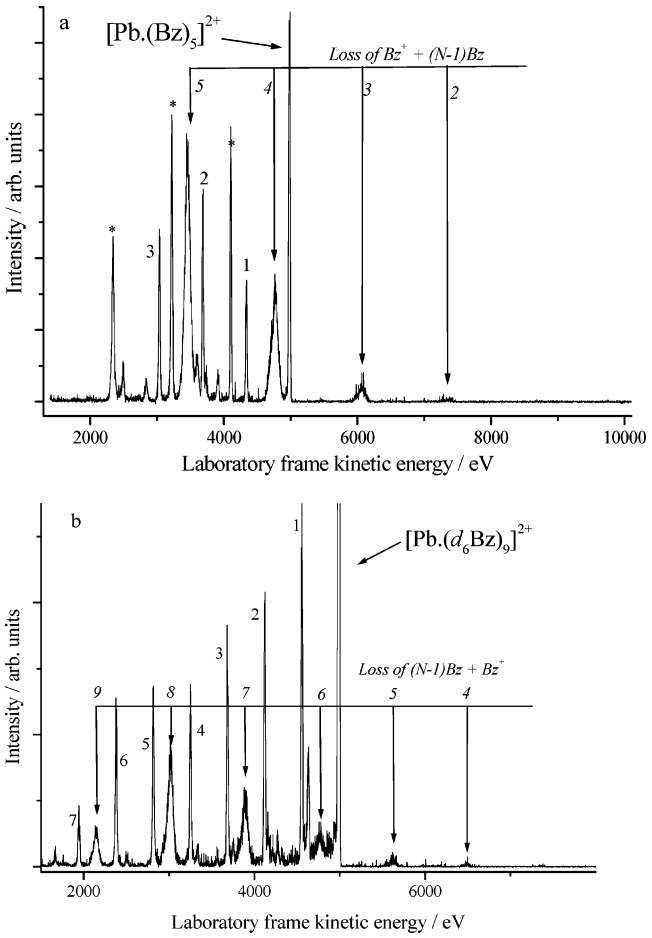

Figure 14. Fragmentation patterns recorded for (a) $[Pb(benzene)_5]^{2+}$ and (b) $[Pb(benzene\text{-}d_6)_9]^{2+}$ following collisional activation.

triply charged clusters of benzene molecules.[55] As might be expected from the distribution of ion intensities, the intensities of neutral loss peaks decline rapidly once $[Pb(Bz)_2]^{2+}$ is formed.

Conclusion

We have shown that it is possible to use a pickup technique to prepare stable complexes between Pb^{2+} and a wide range of ligands. In many instances, the relative intensities of the ions observed follow a pattern very similar to that identified by Shimoni-Livny et al.[10] from a compilation of condensed-phase coordination numbers. Ion intensities for $[Pb(L)_N]^{2+}$ complexes frequently exhibit two maxima at $N = 3-4$ and $6-7$ and a minimum at ~ 5. Compared with other cations with second ionization energies of a similar magnitude, complexes associated with lead appear to exhibit significantly less reactivity when they undergo charge transfer. A possible explanation for such behavior might be the way in which the coulomb repulsion is partitioned between kinetic, intermolecular, and intramolecular internal excitation. It is frequently assumed that a significant fraction of the repulsive energy is channeled into relative kinetic energy of the fragments, a fact that is often used to estimate the separation between positive charges at the instance of fragmentation. However, it is also well-known from neutral kinetics that the shape of a potential energy surface associated with an exothermic process can have a very strong influence on how energy is partitioned into other degrees of freedom.[56] Thus, a reaction barrier that appears toward the product end of reaction coordinate (late barrier) leads to enhanced kinetic energy in the fragments, whereas an early barrier results in a significant fraction of the exothermicity being channeled into internal excitation. The influence of intramolecular energy partitioning have been seen previously in CID experiments on doubly and triply charged clusters ions, where a correlation was observed between increased numbers of vibrational degrees of freedom in the constituent molecules and a decrease in relative kinetic energy of the fragments. In terms of what is observed here for Pb^{2+} in comparison with, for example, Mn^{2+},[28,29] it is quite possible that reactions of the latter proceed on a potential energy surface that promotes intramolecular excitation. In contrast, the lack of reactivity on the part of Pb^{2+} with respect to many of the ligands discussed here may be due to the presence of a barrier that enhances kinetic or intermolecular excitation. Calculations on $[Pb(H_2O)_4]^{2+}$ show that the very high level of reactivity seen in Pb(II)/water complexes (hydrolysis) is due to the presence of an early (and low) reaction barrier to proton transfer.

Evidence of intermolecular excitation is to be seen from the fact that charge transfer is frequently accompanied by the complete loss of all ligands from the product Pb^+ ion. A contributing factor to such behavior could be that the binding energies of these ligands to Pb^+ are low; however, existing solvation enthalpy measurements do not support that assumption.[57] The group of ligands that exhibit the highest degree of reactivity appear to be that where sulfur is involved. Within this group there appears to be a distinction between sp^2 and sp^3 sulfur, with the former in the case of CS_2 being unable to stabilize Pb^{2+}. Such a difference in behavior may reflect the fact that sp^3 sulfur is sufficiently soft as to form a bond with Pb(II) that has a high degree of covalency.

Acknowledgment. The authors thank EPSRC for financial assistance with the experimental program and for the award of studentships to B.J.D. and D.C. We also thank Prof. J. F. Nixon and Dr. M. D. Francis for providing a sample of *tert*-butylphosphaalkyne.

References and Notes

(1) Sigel, H.; Fischer, B. E.; Farkas, E. *Inorg. Chem.* **1983**, *22*, 925.
(2) Tajimir-Riahi, H. A.; Langlais, M.; Savoie, R. *Nucleic Acids Res.* **1988**, *16*, 751
(3) Abu-Dari, K.; Hahn, F. E.; Raymond, K. N. *J. Am. Chem. Soc.* **1990**, *112*, 1519.
(4) Claudio, E. S.; Godwin, H. A.; Magyar, J. S. *Prog. Inorg. Chem.* **2003**, *51*, 1.
(5) Brown, R. S.; Hingerty, B. E.; Dewan, J. C.; Klug, A. *Nature (London)* **1983**, *303*, 543.
(6) Jaffe, E. K.; Volin, M.; Mayers, C. B. *Biochemistry* **1994**, *33*, 11554.
(7) Jaffe, E. K. *Comments Inorg. Chem.* **1993**, *15*, 67.
(8) Christensen, J. M.; Kristiansen, J. In *Handbook on Metals in Clinical and Analytical Chemistry*; Seiler, H. G., Sigel, A., Sigel, H., Eds.; Dekker: New York, 1994; p 425.
(9) Pyykkö, P. *Chem. Rev.* **1988**, *88*, 563.
(10) Shimoni-Livny, L.; Glusker, J. P.; Bock, C. W. *Inorg. Chem.* **1998**, *37*, 1853.
(11) Sidgwick, N. V.; Powell, H. M. *Proc. R. Soc. London* **1940**, *A176*, 153.
(12) Stace, A. J.; Walker, N. R.; Firth, S. *J. Am. Chem. Soc.* **1997**, *119*, 10239.
(13) Walker, N. R.; Wright, R. R.; Stace, A. J. *J. Am. Chem. Soc.* **1999**, *121*, 4837.
(14) Walker, N.; Dobson, M. P.; Wright, R. R.; Barran, P. E.; Murrell, J. N.; Stace, A. J. *J. Am. Chem. Soc.* **2000**, *122*, 11138.
(15) Walker, N. R.; Wright, R. R.; Barran, P. E.; Murrell, J. N.; Stace, A. J. *J. Am. Chem. Soc.* **2001**, *123*, 4223.
(16) Wright, R. R.; Walker, N. R.; Firth, S.; Stace, A. J. *J. Phys. Chem. A* **2001**, *105*, 54.
(17) Salpin, J.-Y.; Tortajada, J. *J. Phys. Chem. A* **2002**, *107*, 2943.
(18) Salpin, J.-Y.; Tortajada, J. *J. Mass Spectrom.* **2002**, *37*, 379.
(19) Winkel, J. F.; Jones, A. B.; Woodward, C. A.; Kirkwood, D. A.; Stace, A. J. *J. Chem. Phys.* **1994**, *101*, 9436.

(20) Cooks, R. G.; Beynon, J. H.; Caprioli, R. M.; Lester, G. R. *Metastable Ions*; Elsevier: Amsterdam, 1973.
(21) Walker, N. R.; Wright, R. R.; Barran, P. E.; Cox, H.; Stace, A. J. *J. Chem. Phys.* **2001**, *114*, 5562.
(22) Seidel, S.; Seppelt, K. *Science (Washington, DC)* **2000**, *290*, 117.
(23) Kohler, M.; Leary, J. A. *Int. J. Mass Spectrom. Ion Processes* **1997**, *162*, 17.
(24) Kohler, M.; Leary, J. A. *J. Am. Soc. Mass Spectrom.* **1997**, *8*, 1124.
(25) Seto, C.; Stone, J. A. *Int. J. Mass spectrum. Ion Processes* **1998**, *175*, 263.
(26) Shvartsburg, A. A.; Wilkes, J. G.; Jackson, O. L.; Siu, K. W. M. *Chem. Phys. Lett.* **2001**, *350*, 216.
(27) Shvartsburg, A. A.; Wilkes, J. G. *J. Phys. Chem. A* **2002**, *106*, 4543.
(28) Shvartsburg, A. A. *Chem. Phys. Lett.* **2003**, *376*, 6.
(29) Walker, N. R.; Wright, R. R.; Stace, A. J. To be submitted for publication.
(30) Duncombe, B. J.; Stace, A. J. To be submitted for publication.
(31) Akibo-Betts, G.; Barran, P. E.; Puskar, L.; Cox, H.; Stace, A. J. *J. Am. Chem. Soc.* **2002**, *124*, 9257.
(32) Cox, H.; Stace, A. J. *J. Am. Chem. Soc.* **2004**, *126*, 3939.
(33) Shi, T.; Orlova, G.; Guo, J.; Bohme, D. K.; Hopkinson, A. C.; Siu, K. W. M. *J. Am. Chem. Soc.* **2004**, *126*, 7975.
(34) Allen, F. H.; Bellard, S.; Brice, M. D.; Cartwright, B. A.; Doubleday, A.; Higgs, H.; Hummelink, T.; Hummelink-Peters, B. G.; Kennard, O.; Motherwell, W. D. S.; Rodgers, J. R.; Watson, D. G. *Acta Crystallogr.* **1979**, *B35*, 2331.
(35) Woodward, C. A.; Dobson, M. P.; Stace A. J. *J. Phys. Chem. A* **1997**, *101*, 2279.
(36) Puskar, L.; Barran, P. E.; Wright, R. R.; Kirkwood, D. A.; Stace, A. J. *J. Chem. Phys.* **2000**, *112*, 7751.
(37) Puskar, L.; Cox, H.; Goren, A.; Aitken, D. C.; Stace, A. J. *Faraday Discuss.* **2003**, *124*, 259.
(38) Akibo-Bettsa, G.; Barran, P. E.; Stace, A. J. *Chem. Phys. Lett.* **2000**, *329*, 431. See ref 28 for a reassessment of the assigned fragmentation patterns.
(39) Abu-Dari, K.; Hahn, F. E.; Raymond, K. N. *J. Am. Chem. Soc.* **1990**, *112*, 1519.
(40) Abu-Dari, K.; Karpishin, T. B.; Raymond, K. N. *Inorg. Chem.* **1993**, *32*, 3052.
(41) Payne, J. C.; ter Horst, M. A.; Godwin, H. A. *J. Am. Chem. Soc.* **1999**, *121*, 6850.
(42) Rue, C.; Armentrout, P. B.; Kretzschmar, I.; Schroder, D.; Schwarz, H. *Int. J. Mass Spectrom.* **2001**, *210/211*, 283, and references therein.
(43) Zhou, M.; Andrews, L. *J. Phys. Chem. A* **2000**, *104*, 4394.
(44) Jiang, N.; Zhang, D. *Chem. Phys. Lett.* **2002**, *366*, 253.
(45) Pandey, K. K. *Coord. Chem. Rev.* **1995**, *140*, 37.
(46) Jeung, G.-H. *Chem. Phys. Lett.* **1995**, *237*, 65.
(47) Sakaki, S.; Kitaura, K.; Morokuma, K. *Inorg. Chem.* **1982**, *21*, 760.
(48) Huheey, J. E.; Keiter, E. A.; Keiter, R. L. *Inorganic Chemistry*; Harper Collins: New York, 1993.
(49) Harris, S. *Organometallics* **1994**, *13*, 2628.
(50) Harris, S. *Polyhedron* **1997**, *16*, 3219.
(51) Nakajima, A.; Kaya, K. *J. Phys. Chem. A* **2000**, *104*, 176.
(52) Gerhards, M.; Thomas, O. C.; Nilles, J. M.; Zheng, W.-J.; Bowen, K. H. *J. Chem. Phys.* **2002**, *116*, 10247.
(53) Koyanagi, G. K.; Bohme, D. K. *Int. J. Mass Spectrom.* **2003**, *227*, 563.
(54) Dillon, K. B.; Mathey, F.; Nixon, J. F. *Phosphorus: The Carbon Copy*; Wiley: London, 1998; p 42.
(55) Gotts, N. G.; Lethbridge, P. G.; Stace, A. J. *J. Chem. Phys.* **1992**, *96*, 408.
(56) Levine, R. D.; Bernstein, R. B. *Molecular Reaction Dynamics and Chemical Reactivity*; Oxford University Press: Oxford, U.K., 1987.
(57) Guo, B. C.; Castleman, A. W., Jr. *Int. J. Mass Spectrom. Ion Processes* **1990**, *100*, 665.